Broadband coherent emission observed in polycrystalline CdSSe nanowires under high excitation

2009 J. Phys.: Condens. Matter 21 375302

(http://iopscience.iop.org/0953-8984/21/37/375302)

J. Phys.: Condens. Matter **21** (2009) 375302 (6pp) doi:10.1088/0953-8984/21/37/375302

Broadband coherent emission observed in polycrystalline CdSSe nanowires under high excitation

R B Liu[1,2], J H Cao[3], Z A Li[4], Q Wang[2], Q L Zhang[2], P B He[2], B S Zou[1,2] and A L Pan[2,5]

[1] School of MSE, Beijing Institute of Technology, Beijing 100081, People's Republic of China
[2] Key Laboratory for Micro-Nano Optoelectronic Devices of Ministry of Education and Micro-Nanotechnology Research Center, Hunan University, Changsha 410082, People's Republic of China
[3] Technical Institute of Physics and Chemistry, Chinese Academy of Science, Beijing 100190, People's Republic of China
[4] Experimental Physics, University of Duisburg–Essen, Duisburg D-47048, Germany

E-mail: Anlian.pan@gmail.com

Received 30 March 2009, in final form 4 August 2009
Published 19 August 2009
Online at stacks.iop.org/JPhysCM/21/375302

Abstract
Polycrystalline CdSSe nanowires were prepared with a low-temperature physical evaporation method. Structural analysis combining HRTEM with XRD demonstrate that these as-prepared wires have a hexagonal wurtzite structure with a polycrystalline nature. Locally excited optical measurements show that though these wires can still act as waveguide cavities, their polycrystalline nature will induce a significant redshift of the emitted light during its transportation along them. Power dependent photoluminescence measurement shows that these polycrystalline wires can achieve broadband coherent emission at the band-edge band under high excitation, which shows marked contrast with the much narrower and multimode spectra observed in the single-crystalline nanowires with the same elemental composition. Time-resolved photoluminescence further confirms the occurrence of coherent emission in these wires, which originates from the electron–hole plasma (EHP) recombination of high-density carriers generated under high excitation. These kinds of polycrystalline alloy nanowires with broadband coherent emission should have potential uses in nano-scaled wavelength tunable light-emitting devices.

(Some figures in this article are in colour only in the electronic version)

1. Introduction

The wide range of potential applications for building up optical integrated microsystems and optical-electronic devices has stimulated great interest in the research of one-dimensional (1D) semiconductor nanostructures, which can be used as both individual device elements and interconnects [1–5]. In particular, such nanostructures can work as a 1D cavity to achieve optical gain and induce coherent emission (lasing) under high excitation [6, 7]. Recently, even tunable lasing across a large spectrum range (from 500 to 700 nm) has been observed in a small single chip using CdSSe nanowires [8]. As we know, almost all of the reported gain or lasing behaviors are in high quality single-crystalline nanostructures [9–12]. However, due to the difference of growth route or condition, polycrystalline nanowires can also be obtained. For example, nanowires prepared using the electrodeposition route are almost all polycrystalline [13, 14]. Even using the high-temperature chemical vapor deposition (CVD) or thermal evaporation route, nanowires grown in the low-temperature zone are usually of poor crystallization or polycrystalline. To get a comprehensive understanding of the optical behavior of semiconductor nanowires under high excitation, it is also

[5] Author to whom any correspondence should be addressed.

necessary to study the optical behavior of polycrystalline nanowires, and to make comparisons with those of single-crystalline wires.

In this work, polycrystalline CdSSe nanowires were prepared using a low-temperature deposition CVD route. Their optical waveguide behavior and light emission properties under different excitations were investigated, and compared with those of single-crystalline wires with the same composition/bandgap. The results show that these polycrystalline wires can also give coherent emission under dense laser excitation, with their emission band much broader than that of the single-crystalline wires. This kind of super-broad coherent emission may find applications in tunable laser sources or white emitting devices.

2. Experimental details

The polycrystalline CdSSe nanowires were prepared using an Au-catalyzed thermal evaporation route similar to that for growing single-crystalline CdSSe nanowires [15], but under a relative low evaporation/deposition temperature. The evaporation/deposition temperature for the polycrystalline wires is 700/380 °C, while the evaporation/deposition temperature for the single-crystalline wires is 900/450 °C. The composition of the polycrystalline wires was kept the same as that of the single crystal wires used for comparative experiments in this work, by adjusting the molar ratio (CdS/CdSe) of the source powder. The morphologies and the energy dispersive x-ray spectrum (EDS) of these CdSSe nanowires were observed with a scanning electron microscopy (SEM, Hitachi S-5200). The high-resolution image of the sample was collected in a high-resolution transmitted electron microscope (HRTEM, Phillips FEG-CM 200). Powder x-ray diffraction (XRD) data were obtained by a Japan Rigaku D/MAX-2400 type diffractometer equipped with graphite-monochromatized Cu Kα radiation ($\lambda = 1.541\,78$ Å).

The waveguide properties of these polycrystalline wires were taken on a scanning near-field optical microscope (Alpha, Witec), equipped with a high-resolution charge coupled device (CCD) camera for acquiring the far-field emission image. A single nanowire was illuminated at its midpoint with a tightly focused laser beam (442 nm line of He–Cd CW laser). The power dependent photoluminescence (PL) and PL dynamics were obtained by femtosecond (fs) laser excitation, which originated from a regenerative amplifier (Spitfire, Spectra Physics) seeded by a mode-locked Ti–sapphire laser (Tsunami, Spectra Physics) with the laser pulse at 800 nm (~120 fs, 0.7 mJ, 1 kHz). It was frequency doubled in a beta-barium borate (BBO) crystal to generate the second harmonic at 400 nm. Then it passed through another BBO crystal, in which the mixing signal was generated at 266 nm. A variable neutral-density filter was used in front of the first BBO crystal to adjust the output energy. The micro-PL of these nanowires was collected by an objective with NA ~ 0.8 (X100) installed in a confocal microscopic system, then focused into a monochromator with an entrance slit width of 10 μm and acquired by a CCD detector (Spectrapro 2300i, Acton). The time-resolved spectra were measured by a photon counting streak camera (Hamamatsu C2909), the time resolution is 20 ps.

3. Results and discussion

The SEM image of the polycrystalline CdSSe nanowire sample shown in figure 1(a) indicates that the wires have lengths from several tens of micrometers to several hundreds of micrometers and widths in between 100 and 500 nm. The *in situ* EDS of the nanowires (inset of figure 1(a)) shows that the sample contains only elemental S, Se and Cd, and the ratio of Cd:S:Se is around 0.49:0.33:0.18. Figure 1(b) is the HRTEM image of a representative wire (inset, the corresponding low-resolution morphology image), which indicates that the wires are polycrystalline with obvious defects and lattice disorder. Figure 1(c) shows the XRD patterns of the as-prepared polycrystalline CdSSe nanowires (upper one) and the single crystal CdSSe nanowires (lower one) for comparison, respectively. It is clearly seen that both samples are hexagonal wurtzite structure, with all their diffraction peaks at the same positions. This result indicates that these two CdSSe samples have the same lattice parameters. According to Vegard's law for ternary CdS_xSe_{1-x} compounds [16], the lattice parameters have a linear dependence on the composition x, according to $c(x) = x \times c\mathrm{CdS} + (1-x)c\mathrm{CdSe}$, where cCdS, cCdSe, and $c(x)$ are the respective c-axis lattice constants of the hexagonal structured CdS, CdSe, and CdS_xSe_{1-x}. From the above analysis, the polycrystalline nanowires have the same alloy composition x as that of the single-crystalline wires, with the calculated x value as 0.6. This value is in good agreement with that obtained from the EDS analysis. The slight broadening of the diffraction peaks for the polycrystalline nanowires originates from the lattice disorder nature of the sample.

Figure 1(d) shows the typical far-field PL image of a single polycrystalline CdSSe wire excited at the midpoint with a focused laser, which exhibits two bright emission spots at the wire ends. The large bright facula in the middle of the wire originates from the *in situ* PL. A portion of the resulting PL was propagated through the wire and emitted at its ends with considerable PL intensity, indicating these polycrystalline wires can still form optical waveguide cavities. The color of the *in situ* PL at the middle part is orange, while the light color at the tips turns to red. This apparent redshift originates from the large amount of trap states or surface states existing in these polycrystalline wires [17].

Figure 2(a) shows the power dependent PL spectra of the polycrystalline wires under different pump fluences. The PL spectrum consists of two emission bands. One locates at 600 nm denoted by P_1, and the other one locates at a low energy emission band at 640 nm denoted by P_2. The band P_1 corresponds to the conduction-band and valence-band transition, which is consistent with the bandgap value of single-crystalline $CdS_{0.6}Se_{0.4}$ nanobelts (2.1 eV) [18]. The P_2 band should originate from trap state or surface trap state recombination [19, 20], similar to the reported results observed in CdSSe doped glass [19, 21].

At low pump fluence (<38 μJ cm^{-2}), the band P_2 is dominant and increases with rising pump fluence, whereas

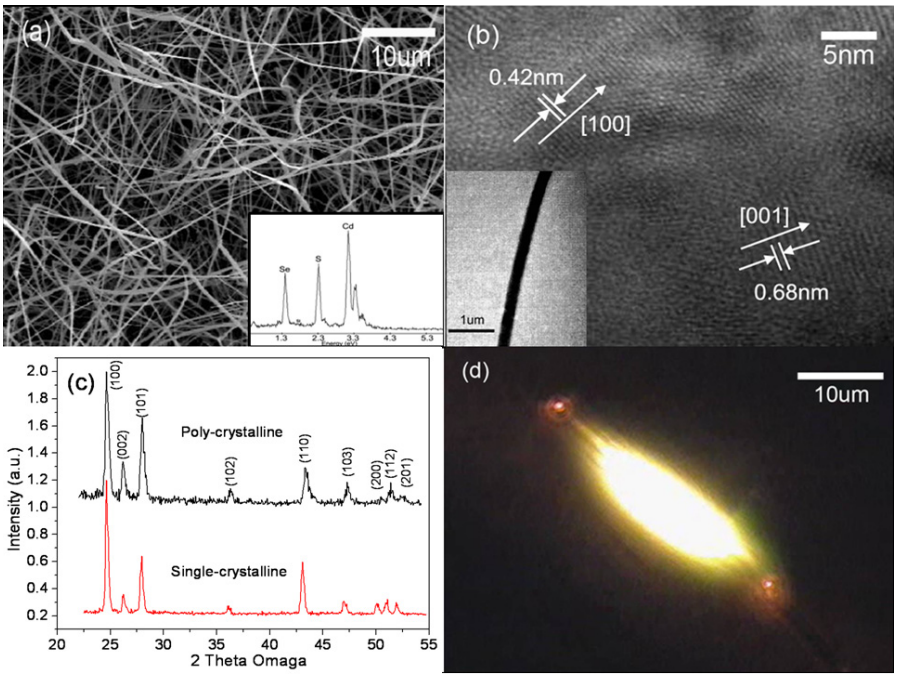

Figure 1. (a) SEM image and EDS of the as-grown polycrystalline CdSSe nanowires. (b) The HRTEM image and the corresponding TEM morphology image (inset) of a representative polycrystalline wire. (c) The x-ray diffraction patterns of the prepared polycrystalline nanowires (upper) and the single-crystalline nanowires for contrast (lower), respectively. (d) Far-field optical image of a single nanowire under local light excitation.

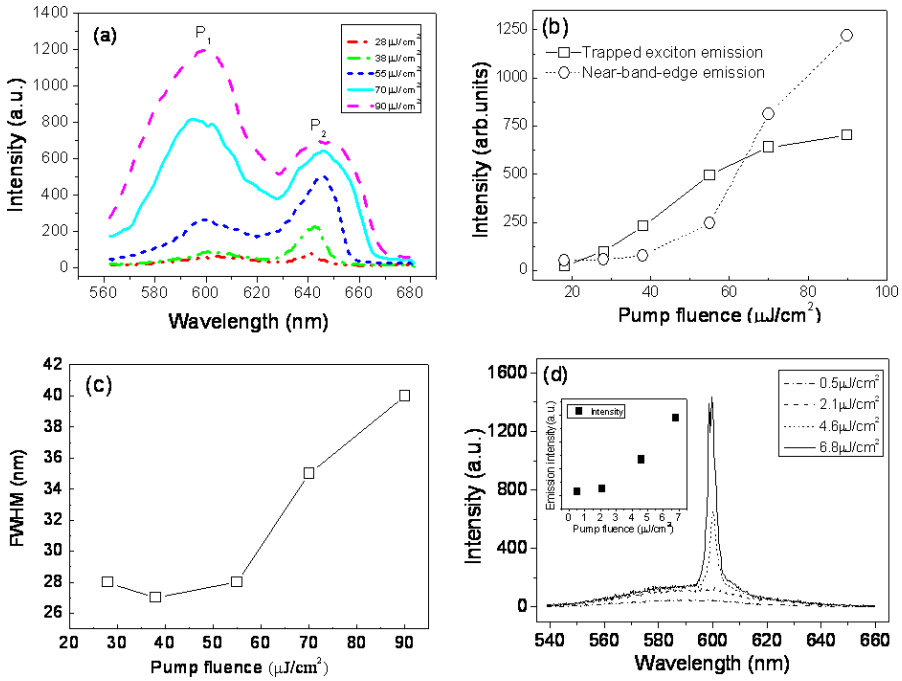

Figure 2. (a) The pump fluence dependent PL of the as-prepared polycrystalline nanowires. P_1 and P_2 denote the high energy band-edge emission band and the low energy trap state related emission band, respectively. (b) The dependence of PL intensity on the pump fluences for the band-edge emission band (circle) and trap state emission band (square) of the polycrystalline CdSSe nanowires, respectively. (c) The pump fluence dependent FWHM of the band-edge emission of the polycrystalline wires. (d) The evolution of PL spectra with pump fluence for the single-crystalline nanowires.

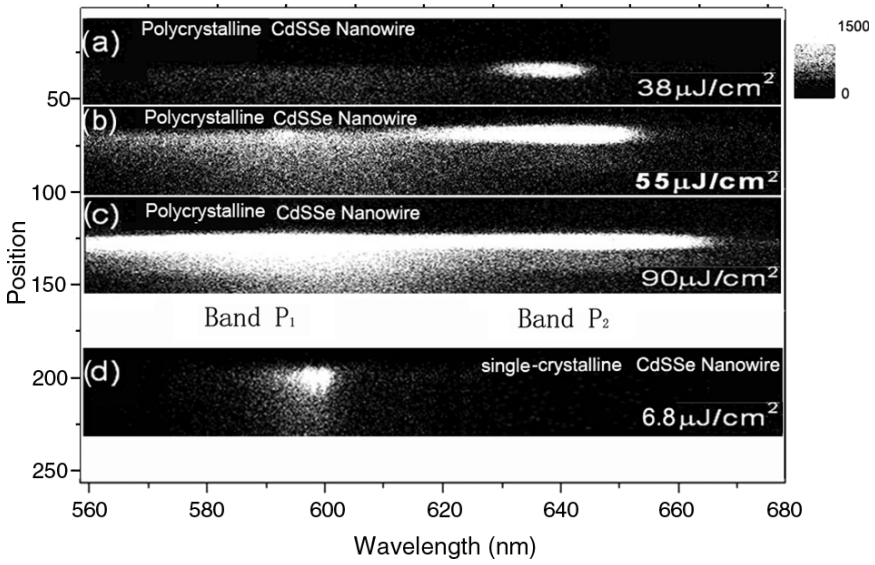

Figure 3. (a)–(c) Two-dimensional far-field PL intensity gray-scale images under pump fluences with 38 μJ cm^{-2} (below the threshold), 55 μJ cm^{-2} (just above threshold), and 90 μJ cm^{-2} (above threshold much more), respectively. (d) The emission image from single-crystalline CdSSe nanowire under a high pump fluence above threshold.

the intensity of the band P_1 shows no significant increase. With the pump fluence increased to ~55 μJ cm^{-2}, the band P_1 shows up, but its intensity is still weaker than that of the band P_2. At even higher fluence (70 μJ cm^{-2}), the intensity of band P_1 becomes higher than the band P_2 and the full-width of half-maximum (FWHM) of P_1 becomes broadened. As the fluence reaches to 90 μJ cm^{-2}, the intensity of band P_2 shows a little increase, indicating the appearance of saturation of the trap state emission under high excitation, while the band P_1 increases drastically with increasing excitation. From the intensity evolution of these two PL bands with the pump fluence, as shown in figure 2(b), it can be found that the saturation effect really occurs on the P_2 band (circle) due to limited density of trap states [22, 23]. While the intensity of P_1 band (square) from band-edge emission has a nonlinear increase with rising pump fluence after the saturation of trap state recombination is reached. Moreover, the FWHM of the P_1 band becomes broader under higher pump fluences, as shown in figure 2(c). In particular, it also exhibits a superlinear increase when the pump fluence is above 55 μJ cm^{-2}, even reaching 44 nm at ~90 μJ cm^{-2}. The broadening with rising pump fluence indicates that it is mainly induced by a high-density carrier effect rather than the composition fluctuation in the wires. Moreover, the P_1 band redshifts from around 597 to 602 nm with the FWHM broadening. The redshift comes from the bandgap renormalization effect due to high-density carrier generation [24]. The superlinear increase of the emission intensity and peak position redshift at band P_1 demonstrate the appearance of amplified spontaneous emission (ASE) in these polycrystalline wires, with a threshold pump fluence of ~50 μJ cm^{-2}. In comparison, the PL spectra of the single-crystalline CdSSe wires (see figure 2(d)) show only band-edge emission, and multimode peaks appear under high excitation. From the dependence of emission intensity on pump fluence (inset of figure 2(d)), the threshold of lasing is at around 2.2 μJ cm^{-2}, which is much lower than that in polycrystalline nanowires (~50 μJ cm^{-2}).

For a more intuitive picture of the PL evolution with the excitation, the two-dimensional gray-scale PL intensity images were measured and are shown in figure 3. The vertical and horizontal axes correspond to the relative position in detector and emission wavelength, respectively. Figures 3(a)–(c) give the intensity images measured from these polycrystalline nanowires under three different pump fluences, (a) 38 μJ cm^{-2}, below the threshold, (b) 55 μJ cm^{-2}, just above the threshold, and (c) 90 μJ cm^{-2}, much further above the threshold. Figure 3(d) gives the intensity image of the contrasting single-crystalline nanowires. Consistent with the observations in figure 2, light in the polycrystalline wires mostly is emitted from the trap state related recombination region (P_2) at a pump fluence lower than the threshold (~50 μJ cm^{-2}), implying that the density of trap states is relatively rich in these nanowires, which is consistent with the observed structure disorder (figure 1(b)) and the exhibited redshift in the far-field PL image (figure 1(d)) [17]. The band-edge emission (P_1) becomes much stronger and wider than that of the trap state emission with rising pump fluence above threshold (see figures 3(b) and (c)), demonstrating the appearance of the broadband coherent emission in the wires. For the single-crystalline nanowires (figure 3(d)) under high excitation, the emission region is concentrated in a very narrow region, showing marked contrast with those polycrystalline nanowires.

For the light emission of the polycrystalline CdSSe nanowires, the intensity evolution of the two bands originates from the process of carrier recombination in the wires. Under excitation, most excited carriers are trapped rapidly (less than 1 ps) by the surface states or trap centers, making the luminescence dominated through the trapped state recombination [25]. In this case, the trapped electrons

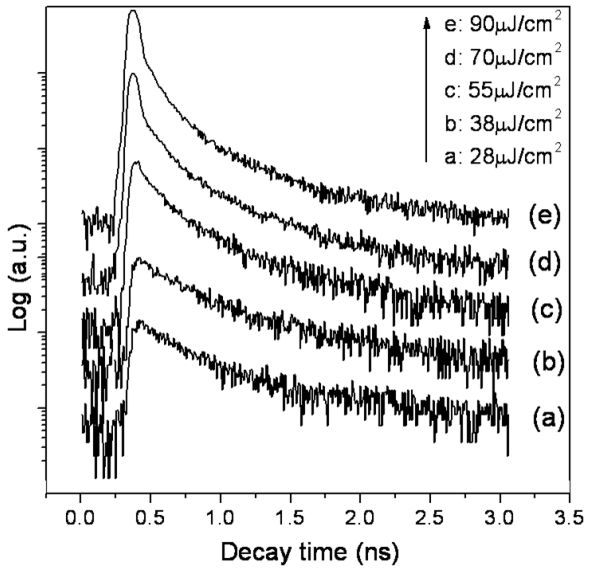

Figure 4. Time-resolved PL of the band-edge emission (P_1) of the polycrystalline wires under different pump fluences.

recombine with holes, giving rise to the band P_2. On increasing the excitation, more electron–hole pairs are excited within the laser pulse width of 120 fs, thus the trapped states are easily filled with these high-density carriers. As soon as the trap states become fully occupied, the trapping process becomes less efficient, and a large number of excited electrons without trapping choose the direct electron–hole recombination (band P_1). The peak P_2 is stronger than the peak P_1 at the beginning of the increasing pump fluence, indicating that recombination through the trapped state is more efficient than direct electron–hole pair recombination at low excitation. While at high excitation, direct free-exciton recombination is more efficient after the saturation of a trapped state appears.

As we know, the superlinear increase of intensity, the band broadening and redshift of the PL emission band at high excitation show clear evidence of EHP formation [24, 26], which indicates that the EHP recombination become the main recombination in these polycrystalline nanowires under higher pump fluences. The broadband coherent emission realized in these polycrystalline wires is quite different from the situation in single-crystalline CdSSe wires, which shows a supernarrow band and multimode occurrence (figure 2(d)) induced by the exciton–exciton/electron–phonon scattering. Exciton–exciton scattering-induced stimulated emission is always narrow. In particular, when it combines with the FP cavity effect, sharp multilasing modes can be generated in single-crystalline nanowires. However, the existence of many trapped carriers in these polycrystalline CdSSe nanowires will strongly influence the occurrence of exciton–exciton collisions, which will induce many electrons and holes to form EHP, and then produce a broadband ASE at high excitation. Although the EHP and cavity effect can bring considerable optical gain in these polycrystalline wires under high excitation, the existing large number of defects and dislocations can dissipate it, making sharp emission or multimode lasing hard to be reached. This broad coherent emission is like the emission situation in the dye solution, but the nanowires are more stable than the dyes.

Table 1. Decay time of the band-edge emission of the polycrystalline nanowires under different pump fluences.

Pump fluence (μJ cm^{-2})	Decay time (ns)	Amplitude (%)
28	$t_s = 0.38$	100
38	$t_s = 0.4$	100
55	$t_s = 0.085$	57
	$t_f = 0.38$	43
75	$t_s = 0.035$	88
	$t_f = 0.25$	12
90	$t_s = 0.026$	90
	$t_f = 0.24$	10

The time-resolved PL under various pump fluence give clear evidence of coherent ASE in the polycrystalline wires. Figure 4 shows the decay curves of the near-band-edge recombination band (P_1), with a pump fluence of 28 μJ cm^{-2}, 38 μJ cm^{-2}, 55 μJ cm^{-2}, 75 μJ cm^{-2}, and 90 μJ cm^{-2}, respectively. The decay curves were fitted well with one or two exponential functions. Table 1 shows the detailed decay time corresponding to different pump fluences. It can be found that the decay process is highly dependent on the pump fluence. At a pump fluence of 28 or 38 μJ cm^{-2}, below the threshold ($\sim$50 μJ cm^{-2}), all decay times fit well to one exponential function with a time constant $\sim$0.4 ns. It corresponds to a exciton-like radiative recombination [27]. As the pump fluence is increased to above the threshold, the decay time fits well to a biexponential function with a fast time constant τ_f and a slow time constant τ_s. The appearance of the fast decay component indicates that a new coherent recombination occurs at high-density carriers. This fast decay time coincides with the EHP recombination [28], indicating the occurrence of coherent EHP recombination under high excitation, which is also in good agreement with the appearance of the broadening and redshift of the PL band. Moreover, with the pump fluence increasing, the fast decay component takes a large proportion in the decay process, which increases from 57% to 90%. The contribution of the fast component increases drastically with increasing pump fluence, indicating that the emission from EHP recombination plays a significant role in the carrier decay process under high excitation.

4. Conclusion

Both polycrystalline and single-crystalline nanowires with the same composition were obtained by a temperature-selected physical evaporation method. The light-emitting properties of these two kinds of wires were comparatively investigated. The results of pump fluence dependent PL and far-field intensity gray-scale images demonstrate that broadband coherent emission can be realized in these polycrystalline alloy nanowires under high excitation, which shows a marked contrast with the much narrower and multimode spectra observed in the single-crystalline wires. The time-resolved PL spectra further confirm the occurrence of coherent emission which results from the formation of EHP recombination in these wires. This interesting optical result indicates that these

polycrystalline CdSSe nanowires may be used as broadband coherent light sources or tunable light-emitting devices.

Acknowledgments

The authors are grateful to the NSF (term nos 90606001 and 50602015) of China and the Hunan Provincial Natural Science Foundation of China (Distinguished Young Scholars) for financial support, and the State Key Laboratory for Structural Chemistry of Unstable and Stable Species, Institute of Chemistry, CAS, for their experimental support.

References

[1] Hu J, Odom T W and Lieber C M 1999 *Acc. Chem. Res.* **32** 435
[2] Law M, Sirbuly D J, Johnson J C, Goldberger J, Savkallv R J and Yang P D 2004 *Science* **305** 1269
[3] Yao Z, Dekker C and Avouris P 2001 *Top. Appl. Phys.* **80** 147
[4] Dai H 2002 *Acc. Chem. Res.* **35** 1035
[5] Huang Y, Duan X and Lieber C M 2005 *Small* **1** 142
[6] Duan X, Huang Y, Argarawal R and Lieber C M 2002 *Nature* **421** 24
[7] Liu R B, Pan A L, Fan H M, Wang F F, Shen Z X, Yang G Z, Xie S S and Zou B S 2007 *J. Phys.: Condens. Matter* **19** 136206
[8] Pan A L, Zhou W C, Leong E S P, Liu R B, Chin A H, Zou B S and Ning C Z 2009 *Nano Lett.* **9** 784
[9] Johnson J C, Yan H Q, Schaller R D, Haber L H, Saykally R J and Yang P D 2001 *J. Phys. Chem.* B **105** 11387
[10] Gargas D J, Toimil-Molares M E and Yang P D 2009 *J. Am. Chem. Soc.* **131** 2125
[11] Agarwal R, Barrelet C J and Lieber C M 2005 *Nano Lett.* **5** 917
[12] Hua B, Motohisa J, Kobayashi Y, Hara S and Fukui T 2009 *Nano Lett.* **9** 112
[13] Zhou S M, Feng Y S and Zhang L 2003 *Euro. J. Inorg. Chem.* **9** 1794
[14] Sarkar J, Khan G G and Basumallick A 2007 *Bull. Mater. Sci.* **30** 271
[15] Pan A L, Yang H, Yu R C and Zou B S 2006 *Nanotechnology* **17** 1083
[16] Perna G, Pagliara S, Capozzi V, Ambrico M and Ligonzo T 1999 *Thin Solid Films* **349** 220
[17] Pan A L, Wang X, He P B, Zhang Q L, Wan Q, Zacharias M, Zhu X and Zou B S 2007 *Nano Lett.* **7** 2970
[18] Pan A L, Yang H, Liu R B, Yu R C, Zou B S and Wang Z L 2005 *J. Am. Chem. Soc.* **127** 15692
[19] Hache F, Klein M C, Ricard D and Flytzanis C 1991 *J. Opt. Soc. Am.* B **8** 1802
[20] Wang Y S, Sun P, Wang Y H, Wang R Z, Zheng D and Li Y L 2003 *Appl. Phys. Lett.* **82** 49
[21] Tomita M 1990 *J. Opt. Soc. Am.* B **7** 1198
[22] Zheng J P, Shi L, Choa F S, Liu P L and Kwok H S 1988 *Appl. Phys. Lett.* **53** 643
[23] Pan A L, Lin X, Liu R B, Li C R, He X B, Gao H J and Zou B S 2005 *Nanotechnology* **16** 2402
[24] Koch S W 1993 *Quantum Theory of the Optical and Electronic Properties of Semiconductors* (Singapore: World Scientific)
[25] Bauer C, Boschloo G, Mukhtar E and Hagfeldt A 2004 *Chem. Phys. Lett.* **387** 176
[26] Klingshirn C 1995 *Semiconductor Optics* (Berlin: Springer)
[27] Tomita M, Matsumoto T and Matsuoka M 1989 *J. Opt. Soc. Am.* B **6** 165
[28] Saito H and Göbel E O 1985 *Phys. Rev.* B **31** 2360